UNIVERSITY OF CALIFORNIA

Los Angeles

High Throughput Screening to Discover Small-Molecule Bacterial Antivirulence Compounds

A thesis submitted in partial satisfaction of the
requirements for the degree Master of Science
in Biochemistry, Molecular and Structural Biology

by

Jason Eddy Gosschalk

2017

ABSTRACT OF THE THESIS

High Throughput Screening to Discover

Small-Molecule Bacterial Antivirulence Compounds

by

Jason Eddy Gosschalk

Master of Science in Biochemistry, Molecular Biology and Structural Biology

University of California, Los Angeles, 2017

Professor Robert Thompson Clubb, Chair

Infections due to antibiotic-resistant bacteria cause tens of thousands of deaths yearly and pose a significant economic and social burden. The need for new classes of antimicrobial drugs is exigent as microbes continue to gain resistance to even the newest and more effective antibiotics. In this thesis, I present the results of a high-throughput screening (HTS) effort to identify small-molecule inhibitors of the Sortase A (SrtA) enzyme. SrtA is a promising drug target that is responsible for decorating the peptidoglycan of Gram-positive bacteria with virulence factors. The newly developed cell-based assay employs the oral bacterium *Actinomyces oris* and was used to interrogate a chemical library of over 200,000 compounds. SrtA inhibitors discovered by HTS are currently being analyzed using secondary assays. A new *Bacillus subtilis* strain has also been created that may be useful in HTS for compounds that inhibit the *Staphylococcus aureus* TarA enzyme. TarA is a N-Acetylmannosamine transferase that catalyzes

the first committed step in wall teichoic acid (WTA) biosynthesis. Inhibitors discovered using this new strain could have useful anti-infective properties.

The thesis of Jason Eddy Gosschalk is approved.

Beth A. Lazazzera

Jorge Z. Torres

Robert Thompson Clubb, Committee Chair

University of California, Los Angeles

2017

Table of Contents

Chapter I: Background and Introduction

Antibiotic-resistant bacteria cause at least 23 million illnesses and 23,000 deaths per year in the United States. Of those deaths, 11,285 are due to Methicillin-resistant *Staphylococcus aureus*, making it a leading cause of healthcare-associated infections and deaths. (Center for Disease Control 2014). In response, alternative targets for antibiotic treatment have been sought in order to treat antibiotic-resistant microbes. Part of this effort has been to develop antimicrobial drugs that mitigate virulence, effectively preventing a microbe's ability to establish infection in a host without affecting cell growth or viability. In this thesis, I present progress toward developing two unique cell-based assays that are designed to identify small molecules that prevent virulence-factor display by *S. aureus*.

Small molecules that impair or reduce bacterial virulence may be promising therapeutic agents as they should enable the host's immune system to clear the infection. An example of such targets for drug development are macromolecular virulence factors that are displayed on the surface of Gram-positive bacteria. Such factors include, among others: pili, lipoteichoic acids (LTA), and wall teichoic acids (WTA) (Comolli 1999, Fittipaldi 2008, Brown S 2013). These molecular structures are not always essential for cell survival, but are frequently required to establish and maintain infection. Thus, eliminating their display can be expected to abate infectiousness but not cell viability outside the host. This dichotomy presents an opportunity to create a class of drugs against which bacteria are less likely to evolve resistance, as only modest selective pressures are imposed outside of the human host. Though conceptually sound, antivirulence drug development has been challenging and no antivirulence drug has thus far been commercialized. Biocompatibility, solubility, and off-target effects pose the most significant challenges in developing drugs. Therefore, there is a significant need for new cell-based

platforms to identify potential antivirulence drugs.

Modern drug-discovery efforts typically employ high-throughput screening (HTS) of compound libraries to identify small molecule lead compounds for further development. HTS is usually performed using either a biochemical or cell-based assay. In biochemical HTS assays, a purified target in a cell-free environment is used and easily detectable and sensitive outputs are available (e.g. colorimetry or fluorescence) to probe the effect of a small molecule on target function. However, HTS biochemical assays can have disadvantages as they do not account for variables such as a small molecule's cytotoxicity, ability to cross the lipid bilayer, or stability in a cellular environment. To compensate for this, cell-based screens are an increasingly popular alternative to identify potential therapeutics. Cell-based screens that use bacterial growth as a metric and have been well validated can be a robust method for screening compound libraries if proper secondary assays are in place to validate that growth inhibition is a result of inhibiting the desired macromolecule or pathway (J. Campbell 2012). These screens must be carefully designed such that they selectively identify only small-molecule inhibitors of the desired target macromolecule or pathway.

The *S. aureus* Sortase A (SrtA) enzyme is an attractive antivirulence drug target. SrtA is a class A sortase that is responsible for the covalent attachment of virulence factors to the cell wall. It is essential for attaching macromolecules such as Protein A, fibrinogen binding clumping-factors, and fibrinonectin-binding proteins (Mazmanian 2001). The absence of virulence factors as a consequence of genetically eliminating *srtA* significantly decreases the infectiousness of *S. aureus* (Mazmanian 2000). Though SrtA is essential for the attachment of virulence factors, neither the SrtA enzyme nor its substrates are essential for cell survival in culture. Unfortunately, the non-essentiality phenotype of SrtA-deficient cells complicates cell-

based assays, as small molecules that inhibit SrtA have not had any effect on *S. aureus* cell growth and it has been difficult to develop cell-based assays that monitor its function. In lieu of using a cell-based assay to discover *S. aureus* SrtA inhibitors, a biochemical assay has been used by the Clubb laboratory and others to execute HTS. The assay involves detecting Förster Resonance Energy Transfer (FRET) activity of a fluorescent substrate that is cleaved by SrtA. The substrate, a FRET pair connected by an LPETG peptide, is hydrolyzed by SrtA between the threonine and glycine residues if the enzyme is not inhibited. Consequently, one of the fluorophores is released and self-quenching ceases, enabling fluorescence detection. Using this assay in HTS and subsequent NMR structure-based studies led to the identification of SrtA-inhibiting pyridizinone molecules (A. H. Chan 2017). This FRET assay has been used by other groups to identify SrtA inhibitors (Cascioferro 2014). Despite its widespread use, no small molecules have been developed further, presumably because they inhibit SrtA poorly or have decreased efficacy in the membranous environment. Thus, no translational inhibitors have been reported and there remains a need for novel discovery methods.

Developing a cell-based SrtA HTS assay for inhibitors has been a challenge as inhibition does not impair *S. aureus* growth in cell culture and because it is difficult to monitor SrtA function in intact cells, as the protein substrates that it displays accumulate in the membrane or non-covalently associate with the cell wall, giving rise to background signals that prevent facile inhibitor detection. Recently, the viability of *Actinomyces ori*s MG-1 was shown to be dependent upon its Sortase A enzyme (^{Ao}SrtA), unlike other microbes characterized to date. The absence of ^{Ao}SrtA in *A. oris* is uniquely lethal due to the buildup of a glycosylated form of the GspA protein (Wu, C. 2014). GspA is glycosylated by the LCP enzyme and ligated to the cell wall by ^{Ao}SrtA (Figure 1). In *A. oris* strains lacking *gspA*, it is possible to remove *srtA* without

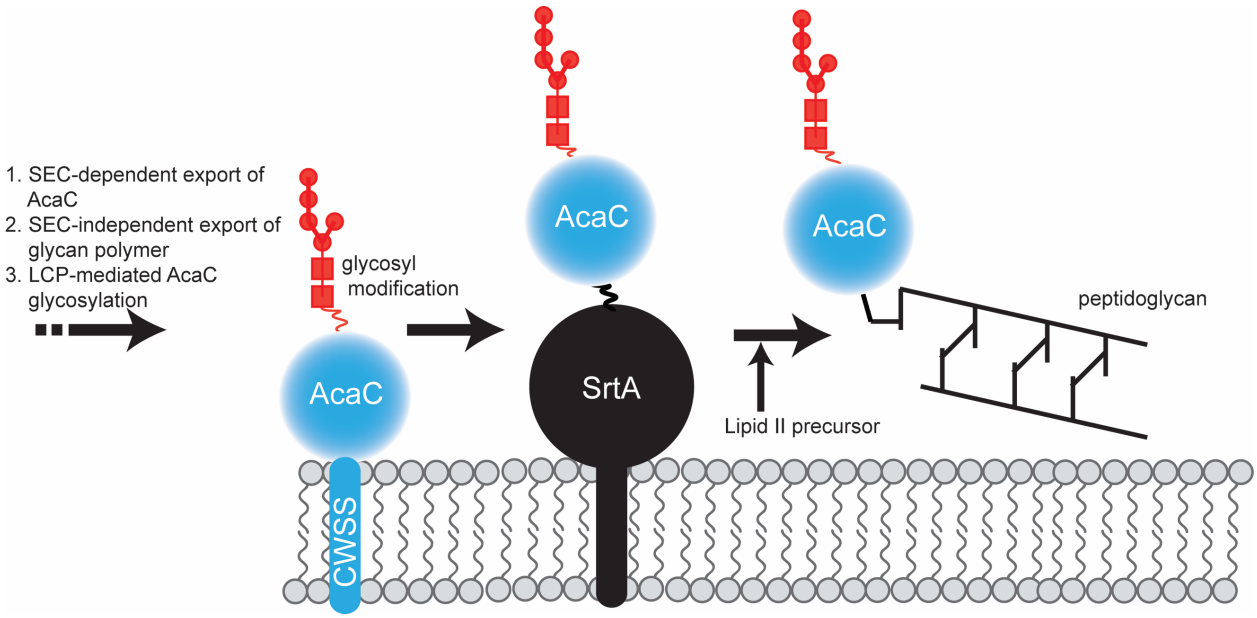

Figure 1: Proposed role for SrtA in *A. oris*. The AcaC protein is exported using the SEC translocon while glycan polymers are exported to the outer cellular membrane via independent transporters. An LCP enzyme transfers the glycopolymer onto the AcaC protein and SrtA hydrolyzes the cell wall sorting signal (CWSS) creating an acyl-enzyme intermediate. AcaC is then transferred to a lipid II precursor and subsequently ligated to the cell wall.

consequence. This conditional lethality offers an opportunity for a novel assay to screen for molecules that inhibit ^{Ao}SrtA by measuring cell viability of the MG-1 strain and a strain lacking both *srtA* and *gspA (ΔsrtAΔgspA)*. A hit molecule is expected to be toxic to the wild type strain and have no effect on the double mutant. As *S. aureus* SrtA and ^{Ao}SrtA share a high degree of sequence homology, it is presumed that inhibitors of ^{Ao}SrtA identified in a cell-based assay will also inhibit *S. aureus* SrtA.

In chapter II of this thesis, I present the development and execution of a useful cell-based high throughput screen that is used to search for small-molecule inhibitors of the ^{Ao}SrtA enzyme. Using this assay, I report the testing of a library of over 200,000 small molecules against *A. oris*, which has identified 2000 lead molecules. Secondary assays are currently being performed to validate preliminary SrtA inhibitors.

The third chapter of this thesis describes efforts to develop a cell-based assay to screen

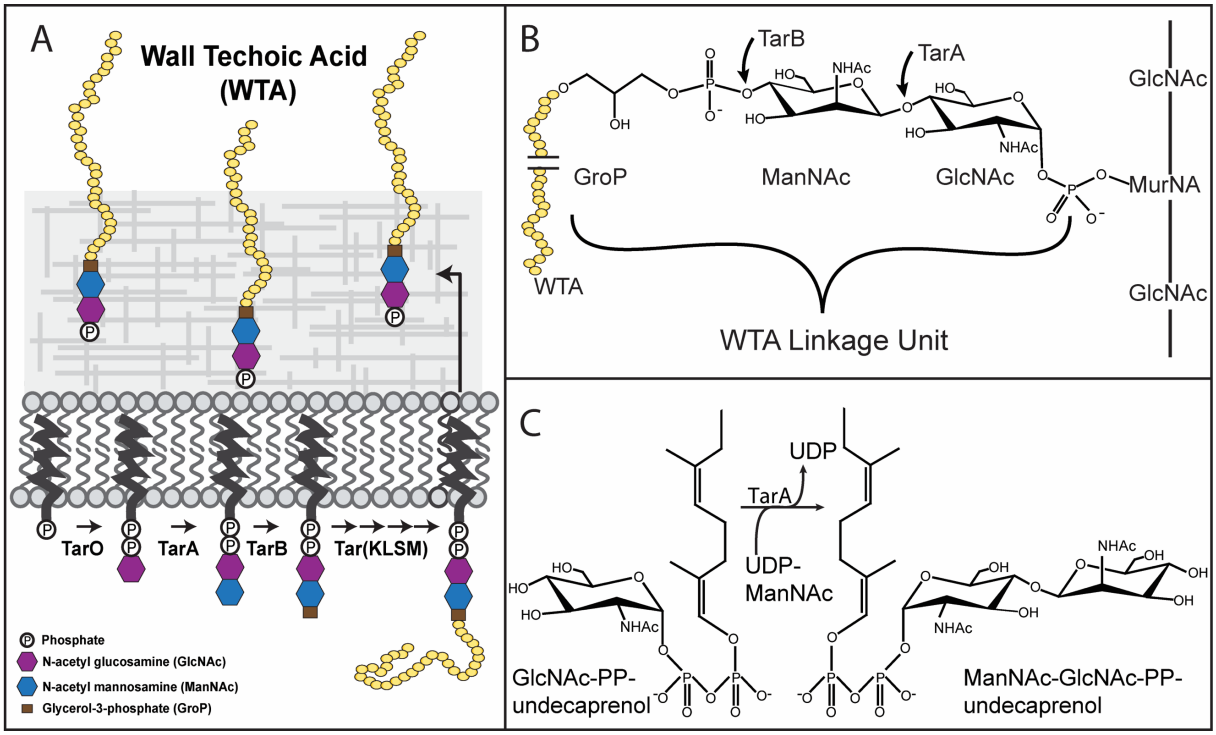

Figure 2: Biosynthesis and structure of WTA. (A) Abbreviated schematic of WTA synthesis, including the first three steps conserved in *B. subtilis* and *S. aureus.* (B) Chemical structure of the WTA linkage unit in both *B. subtilis* and *S. aureus*, indicating linkage unit attachment to the peptidoglycan with the WTA polymer represented by the yellow chain. (C) TarA catalysis of linkage unit synthesis attached to the undecaprenyl lipid moiety that is used in both WTA and cell wall synthesis.

for inhibitors that prevent wall teichoic acid (WTA) biosynthesis. WTA are implicated in crucial processes such as biofilm formation, cation scavenging, and host colonization (Baddiley 1969, Lambert 1975, Marquis 1976, Heckels 1977, Holland 2011, Weidenmaier 2004, Misawa 2015). As such, WTA biosynthetic enzymes are promising targets for the development of antivirulence drugs. WTA biosynthesis occurs on the cytoplasmic face of the plasma membrane using a membrane-anchored precursor undecaprenyl lipid molecule that is shared with peptidoglycan synthesis (Figure 2A) (Bhavsar 2005). After synthesis, WTA is exported to the periplasmic space and covalently bound to the cell wall via a phosphodiester linkage to the C6 hydroxyl of N-acetylmuramic acid (MurNAc). WTA polymers can be chemically diverse, but typically consist of either poly-glycerol chains, synthesized via Tag enzymes (as in *Bacillus subtilis* 168) or poly-

ribitol chains via Tar enzymes (as in *S. aureus* Newman*, B. subtilis* W23) enzymes. Henceforth WTA biosynthesis enzymes will be referred to generally as Tar enzymes for simplicity unless further specification is necessary.

WTA synthesis begins with three conserved reactions and branches after the completion of a common "linkage unit" (Figure 2A). The first enzymatic step in WTA synthesis is the reversible transfer of a N-acetyl glucosamine (GlcNAc) sugar moiety from UDP-GlcNAc to the lipid-anchored undecaprenyl phosphate via TarO. Next, TarA adds a N-acetyl mannosamine (ManNAc) from UDP-ManNAc to the C4-hydroxyl of GlcNAc, resulting in a disaccharide attached to the membrane anchor and completion of the first committed step in WTA assembly (Figure 2C). TarB attaches a phosphoglycerol molecule to the C4 hydroxyl of ManNAc, completing the linkage unit. The linkage unit serves as the anchoring interface between WTA glycopolymers and the murien sacculus (Figure 2B). Its chemical structure is identical in both *B. subtilis* 168 and *S. aureus*. The universality of this linkage unit implicates TarOAB enzymes as promising drug targets with broad-spectrum efficacy.

WTA biosynthetic enzymes can be classified as antivirulence or anti-bacterial targets depending upon where they are located in the pathway. WTA were previously thought to be essential for cell survival, but studies indicate that deletion of early-stage enzymes results in cells lacking WTA that are viable over multiple generations (M. A. D'Elia 2006, M. A. D'Elia 2006, M. A. D'Elia 2009). TarO and TarA are located at the beginning of the pathway and are nonessential for bacterial survival, though their absence causes a disappearance of WTA from the peptidoglycan and a rod-to-spherical morphology change in rod-shaped bacteria like *B. subtilis* (M. A. D'Elia 2009, M. A. D'Elia 2006). In addition, genetic elimination of *tarO* or *tarA* can slow growth; in contrast, TarB and all proceeding enzymes, including the WTA ABC-like

transporter TarGH, are defined by the essential-lethality paradox. Genes coding for these downstream proteins can only be knocked out if either *tarO* or *tarA* is knocked out in parallel. Thus, late-stage enzymes are anti-bacterial targets, while TarO and TarA are targets for antivirulence research because their inhibition does not cause cell death. Interestingly, in addition to preventing WTA synthesis, removing TarO or TarA re-sensitizes methicillin-resistant bacteria to β-lactam antibiotics, making a TarO- or TarA- inhibitory drugs a potentially valuable tool in combinatorial treatments for systemic methicillin-resistant infections (Maki *et. al 1994,* Labroli *et. al* 2016).

Small-molecule inhibitors exist for TarO and TarGH but are unfit for therapeutic use, though they have proven useful in studying this pathway (Schirner 2011, X. P. Wu 2016, Suzuki 2017, Y. G. Chan 2013). Tunicamycin is a naturally derived and characterized small molecule that is known to inhibit enzymes that transfer a hexose-1-phosphate sugar onto membrane-anchored lipid phosphates, with preferential activity toward UDP-GlcNAc transferases. In *S. aureus,* tunicamycin inhibits both TarO and a peptidoglycan biosynthesis enzyme, MraY; however, its affinity for UDP-ManNAc transferases causes preferential inhibition of TarO almost 100 times more effectively than MraY, making it a useful research tool for studying bacterial activity in the absence of WTA (Campbell *et. al* 2011). Tunicamycin broadly inhibits both TagO and TarO in *B. subtilis* and *S. aureus*. Recently, a new class of TarO inhibitors was reported and are referred to as tarocin A and B (Labroli *et. al* 2016). Little is known about tarocin molecules, though they are reported as nitrogen-containing heterocyclic compounds with cell-based EC_{50} values in the nanomolar range.

Inhibitors of late-stage enzymes in WTA production have been discovered by taking advantage of the essential-lethality paradox (Lee 2010, Swoboda 2009). Utilizing the essential-

lethality of the WTA biosynthetic pathway, targocil was observed to inhibit WTA export to the cell surface via inhibition of the TarG enzyme in *S. aureus.* Targocil is bactericidal if applied to a system in which WTA production is otherwise intact and an effective method to prevent WTA surface display (Lee *et. al* 2010). Targocil is selectively active against the *S. aureus* TarGH (^{Sa}TarGH) ABC-like transporter and shows no inhibitory activity against the *homologous B. subtilis* TagGH (^{Bs}TagGH). This is interesting, considering ^{Sa}TarGH indiscriminately exports the poly-glycerol WTA when cloned into a strain of *B. subtilis* lacking its endogenous ^{Bs}TagGH (Schirner *et. al* 2011). To date, there are no known inhibitors of other WTA biosynthetic enzymes that are non-toxic to humans.

The N-acetylmannosamine transferase TarA is one of the most promising targets for drug therapy. Though no catalytic residues have been proposed, *in vitro* biochemical studies have shed insight into the behavior of the TarA homolog in *B. subtilis* TagA (^{Bs}TagA). ^{Bs}TagA shows a preferential substrate recognition for longer-length lipid chains but does not show any discretion in detecting differentially saturated or branched molecules. This observation holds true for modifications to the lipid chain at the reducing end of the substrate near the active site. The kinetic properties of TagA describe an enzyme with a moderately rapid turnover rate of 735 sec^{-1} and a K_m consistent with cellular substrate concentrations (Zhang *et. al* 2006). While there is an abundance of glycosyltransferases that utilize lipid substrates, TarA is predicted to have a novel fold, lending itself to structural and mechanistic properties that may make it uniquely suited as a drug target.

Previous *in vitro* studies purified ^{Bs}TagA for biochemical assays that require expensive substrate and time-consuming protocols, indicating that a simplified system to assess enzyme function is necessary. TarA is not required for cell survival in either *B. subtilis* or *S. aureus*;

however, its absence causes a marked morphological shift in *B. subtilis* from rod to spherical. This cytological characteristic presents a unique opportunity for cell-based screens that utilize cellular morphology as a proxy for enzyme activity. The clinically relevant enzyme, ^{Sa}TarA, is more difficult to study. The loss of WTA due to inactive or absent TarA in *S. aureus* can only be determined biochemically. The need for a convenient and biologically relevant system for testing ^{Sa}TarA functionality is principal.

In the third chapter of this thesis, I present results describing the ongoing development of a system for studying the activity of the ^{Sa}TarA enzyme in its nonnative host *B. subtilis*. I report strain 16802, which relies on ^{Sa}TarA for WTA production. ^{Sa}TarA is ectopically expressed and replaces the N-acetylmannosamine transferase activity of the native ^{Bs}TagA and that activity appears to be sufficient for complete recovery of cell morphology and growth. This strain of *B. subtilis* is a promising opportunity to study ^{Sa}TarA catalytic residues and implement a novel high throughput screen that utilizes *B. subtilis* cell morphology as a readout of ^{Sa}TarA inhibition.

Chapter II: Cell-based HTS for small-molecule inhibitors of the SrtA Enzyme

This chapter describes a novel cell-based assay to screen for inhibitors of the SrtA enzyme. This assay was used in HTS to assess the inhibitory properties of over 200,000 compounds (Figure 3). Approximately 2,000 potential SrtA inhibitors were identified. In the future, these lead molecules will be assessed using secondary assays and structure-activity relationships will be established (Figure 3A).

Results

HTS assay optimization. *Actinomyces oris* strains were assessed for cell growth and sensitivity to 1% dimethyl sulfoxide (DMSO) in 50 µL cultures. Initially, the optimal inoculant concentration was determined. Wells containing 50 µL of media were inoculated at starting

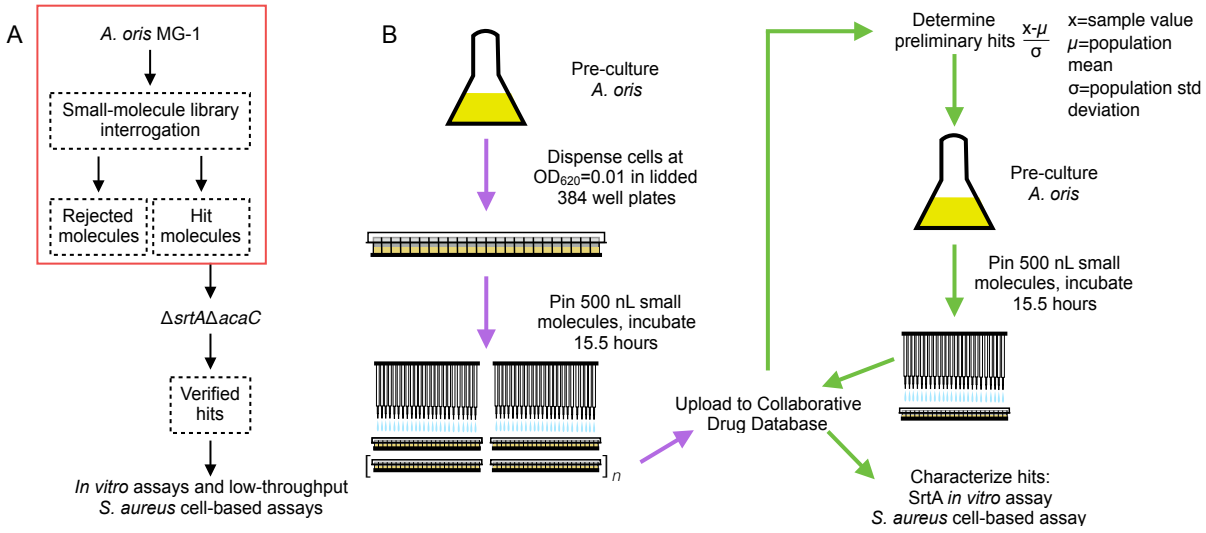

Figure 3: Complete HTS schematic and assay schematic. (A) Schematic of HTS ending in lead compound selection for structure-activity relationship (SAR) experiments. Work completed in this thesis is highlighted with a red box, including screening of over 200,000 molecules against the wild-type *A. oris* MG-1. (B) More detailed schematic of boxed and proceeding step from (A). Pre-cultures are grown to mid-log phase and dilution to a final OD_{620} of 0.01 in the presence of a small molecule. Data is uploaded to an online vault and hits selected for subsequent screening against Δ*srtA*Δ*acaC,* which is being conducted.

densities of OD_{600} = 0.01, 0.005, and 0.001 and grown at 37°C unshaken. *A. oris* strains reach stationary phase at approximately 16 hours when inoculated at an OD_{600} of 0.01 whereas higher dilutions appear to take longer than 18 hours to reach stationary phase and are unrealistic for HTS (Figure 4A). We observed *A. oris* has a doubling time of nearly two hours. Compounds are dissolved in 100% DMSO and final DMSO concentration is expected to be 1% in each well during HTS. We therefore assessed *A. oris* sensitivity to varying levels of DMSO. The Z'-factor was then determined for these cultures (see *Materials and Methods*).

Cultures inoculated at an OD_{600} of 0.01 grown in the presence of DMSO appear to have more desirable Z'-factors than cells grown in the absence of DMSO (Figure 4A). Whereas both the MG-1 and Δ*srtA*Δ*acaC* strains appear to have increased Z'-factors in the presence of 1%

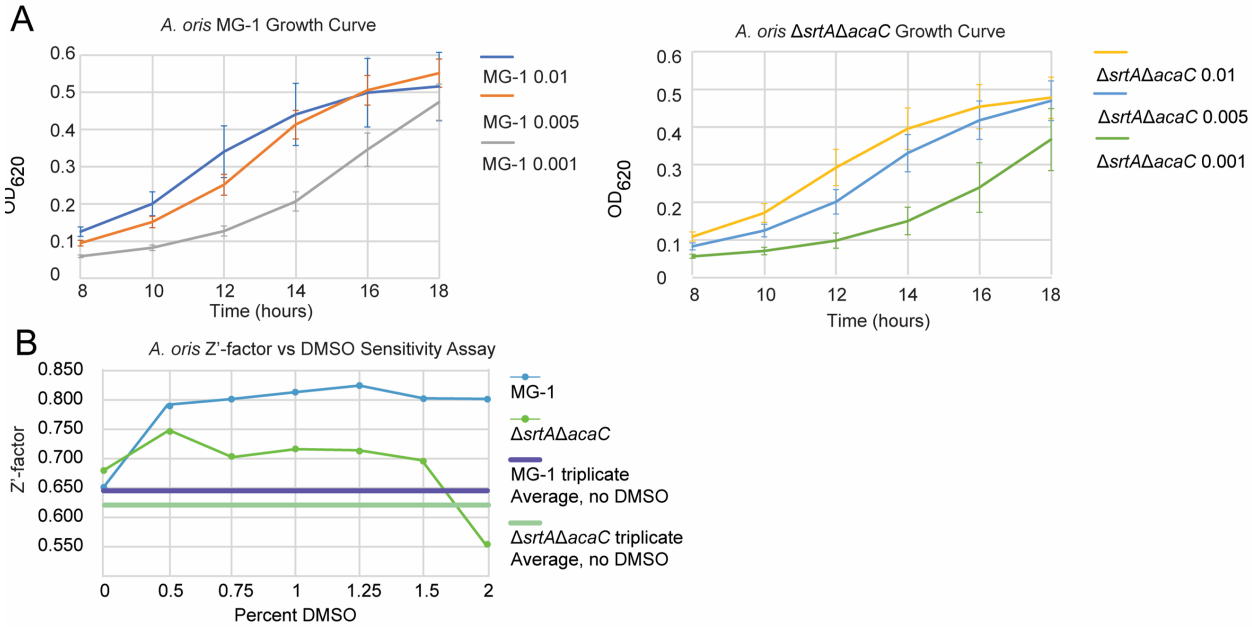

Figure 4: Optimization and growth assays of *A. oris* strains MG-1 and Δ*srtA*Δ*acaC*. (A) Left, strain MG-1 and right, strain Δ*srtA*Δ*acaC*. Growth curve between hours 8 and 18, representing the exponential growth. Optical density was measured every two hours. Cells were grown in 50 µL cultures in a 384-well plate. Error bars represent one standard deviation of 112 discrete wells. (B) Z'-factor for *A. oris* strains grown in the presence of DMSO. Error bars are absent because the Z'-factor is a statistical parameter that represents the standard deviation.

DMSO, the Δ*srtA*Δ*acaC* strain has depreciated assay sensitivity at higher levels of DMSO and the MG-1 strain is unaffected by DMSO up to 2% (Figure 4B). Relative to three-day triplicate data measurements without DMSO, the Z'-factors of both strains of *A. oris* grown in the presence of any DMSO are increased. We conclude that 1% DMSO does not adversely affect *A. oris* and the quality of the assay.

Preliminary testing to verify hit parameters. For HTS, the growth effects of all molecules in the compound libraries will be determined for MG-1. Preliminary hits that inhibit growth will be screened against the Δ*srtA*Δ*acaC* strain of *A. oris*. The parameter for a preliminary hit has been chosen as any molecule that negatively affects growth by more than three standard deviations from the plate average (a Z-score less than -3. See *Materials and Methods).*

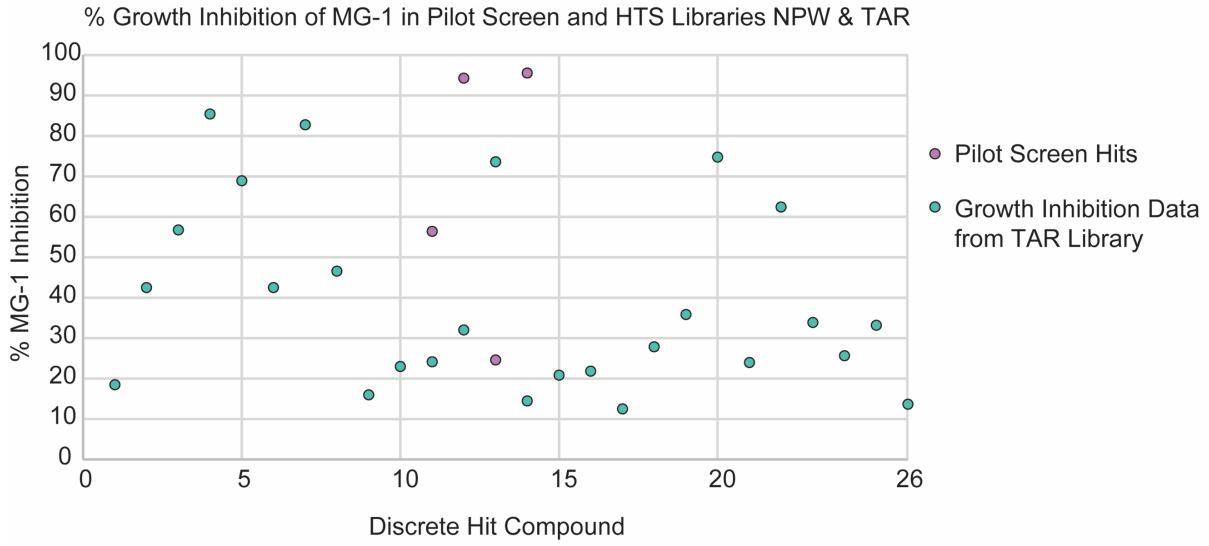

Figure 5: Comparison of data from a pilot screen (NPW library) and HTS (TAR library). The pilot screen, which tested all NPW compounds against both strains, identified hits at various levels of MG-1 growth inhibition relative to the plate negative control. In HTS, TAR hits were identified using a Z-score less than -3 and then % growth inhibition was calculated relative to the plate negative control. Using the Z-score method identifies % inhibition with a sensitivity high enough to satisfy pilot screen standards and streamlines HTS. Growth inhibition is 100-100(sample/control).

A preliminary hit cutoff of Z-score = -3 was validated using a full dataset of growth inhibition against both strains of *A. oris.* Pilot HTS studies were performed using the NPW library. All compounds in the NPW library were tested for their ability to inhibit the growth of the MG-1 and Δ*srtA*Δ*acaC* strains. In the pilot screen, molecules were determined as hits if they selectively inhibited MG-1 growth and not Δ*srtA*Δ*acaC* growth. Pilot screen molecules were hits if they caused 25% or less growth of the MG-1 strain relative to the Δ*srtA*Δ*acaC* strain. Of those hits identified in the pilot screen, the growth inhibition of MG-1 alone was then calculated relative to the plate negative controls. These values were compared to preliminary hits from the TAR library. Preliminary hits were determined from the TAR library using a cutoff of a Z-score of -3 (see *Materials and Methods*). Of these 26 identified TAR preliminary hits, the growth inhibition of MG-1 was calculated relative to the plate negative controls.

MG-1 growth inhibition of "hits" was compared between the NPW pilot screen and TAR library. A preliminary hit Z-score less than -3 detects growth inhibition densities that were flagged as verified hits during the pilot screen, indicating that this hit determination system is appropriate for HTS (Figure 5).

Determination of assay precision. Before complete implementation of HTS, it is essential to assess the reproducibility (precision) of the assay in the presence of compounds and 1% DMSO. Therefore, we screened the TAR library, consisting of 8,640 compounds, against *A. oris* MG-1 three times before completion of the entire 200,000-compound library. Though unconventional for HTS, this triplicate data set was obtained with two runs at hour 18 and one run at hour 15.5. The three TAR runs have preliminary hit rates of 0.625%, 1.157%, and 0.48%, respectively. The three runs altogether share 16 preliminary hits, while the two 18 hour assays share 35 preliminary hits and the 15.5-hour assay shares 18 preliminary hits with each assay

measured at 18 hours (Figure 6). The non-overlapping preliminary hit molecules from the three TAR library assays had Z-scores near -3, indicating that these molecules nearly grew to the average density. Whereas, the "overlapping" preliminary hits had more severe Z-scores, as extreme as -18. The overlap of the more extreme hits (with more negative Z-scores) indicates that this assay is reproducible. From this data, it can be concluded that this cell-based assay reliably reproduces hits across the phenotype-severity spectrum and is appropriate for large-scale HTS.

Ongoing HTS of compound libraries at the MSSR. Using the MG-1 strain, a HTS campaign was performed against 202,880 small molecules. These compounds were assayed for their inhibitory effect on *A. oris* MG-1 growth, with a final hit rate of 1.004%. The majority of compounds have little to no effect on the growth of *A. oris* MG-1 and many hit compounds are no-growth phenotypes. This is illustrated by the bulbous volume in a violin plot (Figure 7A). While cells grow to an average OD_{620} = 0.527 in the presence of inert molecules, there are a number of outliers that fail to

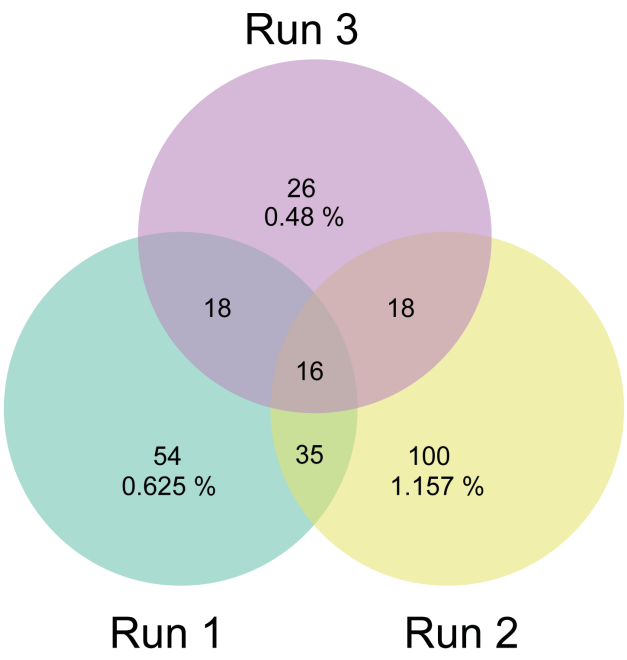

Figure 6: Comparison of run data from the TAR library, which was assayed 3 times. Each circle represents one run with the respective hit rate listed below the total number of hits. Integers in the overlapping regions indicate common hits between repeated runs of the TAR library. Runs 1 and 2 were read after 18 hours of growth and run 3 was read after 15.5 hours.

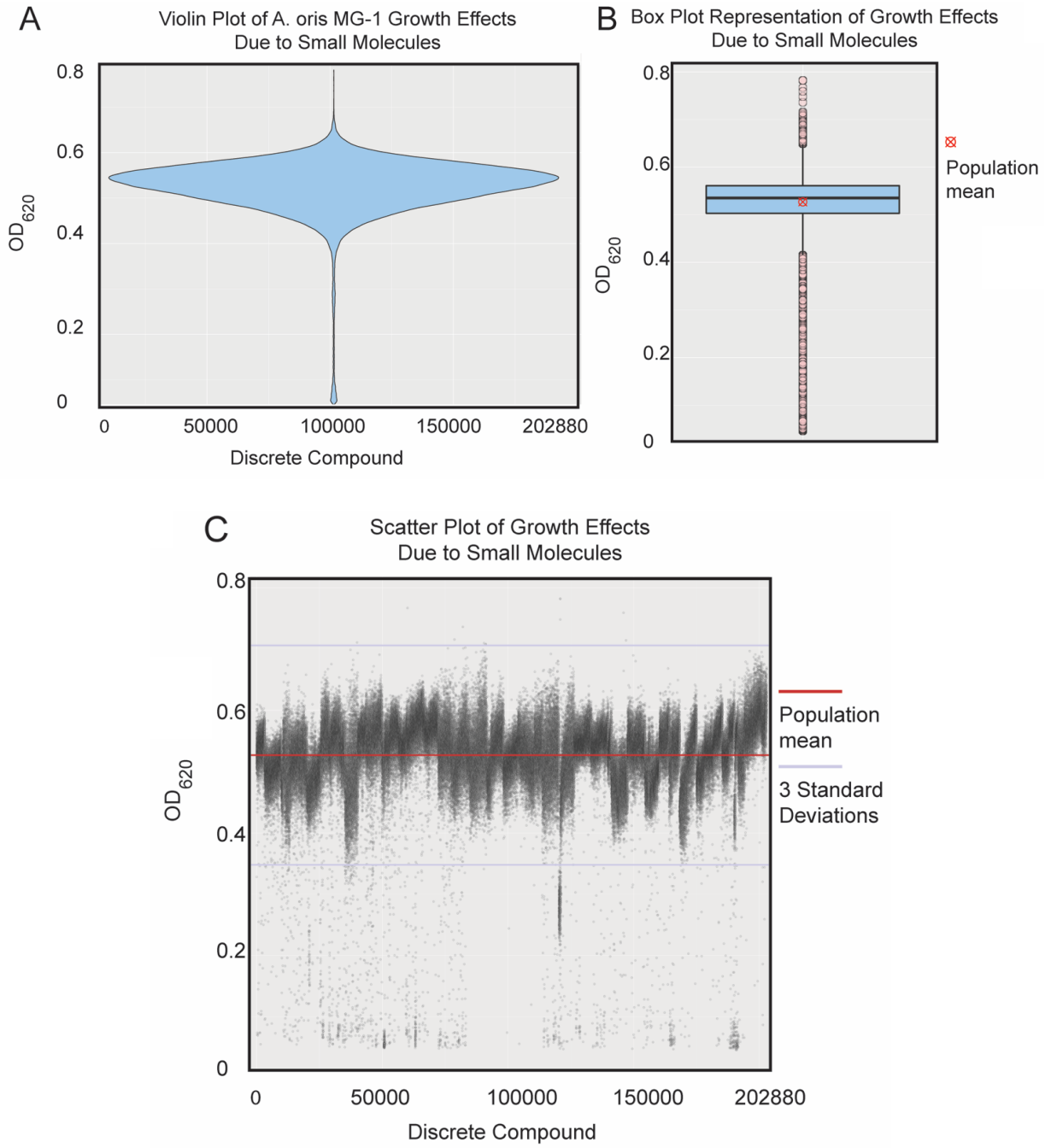

Figure 7: Statistical analyses of compounds screened against *A. oris* MG-1. (A) Violin plot of optical density readings at 620 nm. Most compounds have no effect on growth as the majority of plot area coincides with the population mode and mean as shown in (B), the box plot of all data points. Note that no data points have a reading of "0" as OD_{620} are not normalized. (C) Scatter plot of all data points. Each point represents one discrete compound. Any large gaps in compounds below a Z-score of three (e.g. around 100,000) indicate a library with a lower hit rate.

grow completely (Figure 7B). Compared to growth data from Figure 4A, hit molecules include both bactericidal (no-growth) and growth-slowing phenotypes that were either into the early-exponential phase or not yet into the late-exponential phase (Figure 7C, points below the lavender line). Despite this presence of slow-growth observations, a significant portion of hits are statistical outliers with severe inhibitory effects on growth (Figure 7B). While hits have not been counter-screened for activity against Δ*srtA*Δ*acaC,* this HTS yields a significant but realistic number of molecules for further investigation.

Hits from HTS were compared to data from a previous biochemical HTS completed by the Clubb laboratory using purified *S. aureus* SrtA. Subjecting the data to this filter reveals twelve overlapping compounds that had greater than 50% inhibition of the SrtA enzyme *in vitro* and inhibited MG-1 growth to an OD_{620} Z-score less than -3. We conclude that this enzyme is detecting previously-identified SrtA inhibitors.

Discussion

In this chapter, I report the results of ongoing HTS for inhibitors of the SrtA enzyme. Interestingly, *A. oris* appears to grow to a higher density in the presence of DMSO. While this increases the dynamic range of the assay and is a beneficial effect for HTS, the mechanism of action is unclear. *A. oris* grows in a clumped morphology until late into the exponential growth phase and into the stationary phase of growth. This clumping may have an effect on optical density measurements in 384-well plate formats and it is possible that DMSO is interfering with this clumping and causing a more evenly turbid solution.

Determining hits using a Z-score less than -3 is an effective way to increase efficiency while maintaining the quality and sensitivity of the assay. Pilot screen data indicates that verified

hit compounds may have growth-slowing phenotypes, which are detected using this preliminary hit metric.

Slow-growth phenotypes reiterate the benefit of reading cell density before stationary phase. Waiting until stationary phase to acquire data allows slow-growing cells to continue growing while the unaffected densities have plateaued, decreasing the likelihood of detecting SrtA inhibitors. 15.5 hours is the optimal read time because it is just before cells have reached stationary phase and can detect compounds that are decreasing, but not entirely preventing, growth.

This cell-based assay vigorously and rapidly assesses the effect of small molecules on the growth of *A. oris*. The observed preliminary hit rate of 1.004% is at the upper limit of typical HTS hit rates and can be decreased upon removal of molecules that are known bactericides (e.g. vancomycin derivatives). Further work will include screening these preliminary hit molecules against the Δ*srtA*Δ*acaC* strain followed by an *in vitro* assay testing these molecules against the purified *S. aureus* SrtA enzyme; this will lead to verified hit molecules. After this thorough characterization of verified hit compounds, similar compounds can be purchased, tested and assayed against the *S. aureus* SrtA enzyme. Comparing cell-based HTS data to previous biochemical assays indicates that this screen is identifying compounds that inhibit the SrtA enzyme significantly. The number of molecules that both cause growth defects in *A. oris* and inhibit the SrtA enzyme *in vitro* is expected to be small as cell-based assays are highly specific and can eliminate molecules incompatible with cellular conditions. Thus, a list of 12 molecules that are hits in both assays suggests specificity and the likelihood that this cell-based screen is detecting SrtA inhibitors.

After optimization, molecules identified as verified hits in this assay may mitigate the virulence of Gram-positive bacteria such as *S. aureus* and may become increasingly crucial as overuse and misuse of available therapies ushers in a new pre-antibiotic era. Data from this assay may be used to investigate inhibitors of the SrtA enzyme.

Materials and Methods

Actinomyces oris strains and media. A. oris strains MG-1 and Δ*srtA*Δ*acaC* were obtained from our collaborator (H. Ton-That, University of Texas Health Science Center, Houstan TX). Strains were cultured in Brain-Heart Infusion Broth, Modified (Fisher #B99070) with kanamycin to 50 μg mL^{-1}. 25 mL cultures were grown in 250 mL flasks shaken at 90rpm at 37°C in a sealed incubator.

HTS Optimization. Strains were inoculated at 2 fold dilutions (0.01, 0.005, 0.0001) and allowed to grow for 18 hours. Plates were removed and de-lidded for OD_{620} measurement every two hours between hour 8 and 18. Each measurement removes the plate from the incubator for five minutes. Strains were then assayed against DMSO sensitivity at DMSO concentrations varying between 0% and 2%. Finally, strains were grown in 384-well plates, OD_{620} measurements obtained, and data analyzed for Z'-factor analysis, calculated as previously described (J. C. Zhang 1999). Assays for Z'-factor were conducted on two separate plate readers three total times.

High-throughput Screening. 25 μL fresh BHI was distributed into 384 well plates (E&K Scientific 13062) using a 384-well microplate filling manifold. Kanamycin (50 μg mL^{-1}) was used to prevent contamination and Penicillin G (100 μg mL^{-1}) was used as a positive control (antibiotics were included at 2X concentration (kanamycin, 100 μg mL^{-1}; penicillin, 200 μg mL). 500nL of small molecules dissolved in 100% DMSO were aliquoted into each well. *A. oris* MG-

1 was diluted to an OD_{600} = 0.02 and shaken vigorously to break apart clumps, then 25uL per well was aliquoted to a final cell density of 0.01. The plate setup was as follows: row 1, negative control; row 2, negative control + 1% DMSO; rows 3-22, compound library; row 23, positive control + DMSO; row 24, positive control. Plates were lidded and placed in a humidified incubator at 37°C. After 15.5 hours, plates were removed from the incubator, de-lidded and OD_{620} values measured using an Envision Multilabel Plate Reader (PerkinElmer #2104-0010A). Automation was completed using a Spinnaker Microplate Robot (Thermo #SPK0001). Compound libraries in the UCLA Molecular Screening Shared Resource (MSSR) are chosen by Dr. Robert Damoiseaux for their drug-like properties and include the FDA-approved Drug Library, LOPAC, NIH Clinical Collection, Microsource Spectrum Collection, Druggable Compound Set, Lead-like Compound Set, Combichem Library, and a UCLA in-house Collection.

Data Analysis. Raw data consisted of comma separated value (.csv) files with OD_{620} measurements in plate format. The data were formatted into matrices that correlate plate and well identity with OD_{620}. Basic statistical analyses were performed to identify any plate irregularities. This parsing was completed in-house using a custom program written in C++ (available for open-source use, github.com/jasongosschalk/A.-oris-HTS-Data-Analysis). Formatted data was either uploaded to the Collaborative Drug Database (www.www.collaborativedrug.com) for further analysis or exported for analysis using R (www.r-project.org). Box plot, violin plot, and scatter plot were produced using the ggplot library (www.ggplot2.com). A compound was classified as a "hit" if it decreased cell growth and resulted in a Z-score less than -3, where one unit represents one standard deviation from the average growth of the entire plate, after 15.5

hours of growth. Note that day-to-day variation is accounted for. Hits are determined relative to individual plate statistics, though population statistics are also presented in this thesis.

Chapter III: Construction of *B. subtilis* strains for HTS: strain 16802 utilizes *S. aureus* TarA for wall teichoic acid production

This chapter describes the construction of a novel strain of a *B. subtilis* that relies on the *S. aureus* TarA enzyme for WTA synthesis and its rod-shaped morphology. WTA is an essential surface glyopolymer that contributes to the virulence of *S. aureus*. TarA is a N-

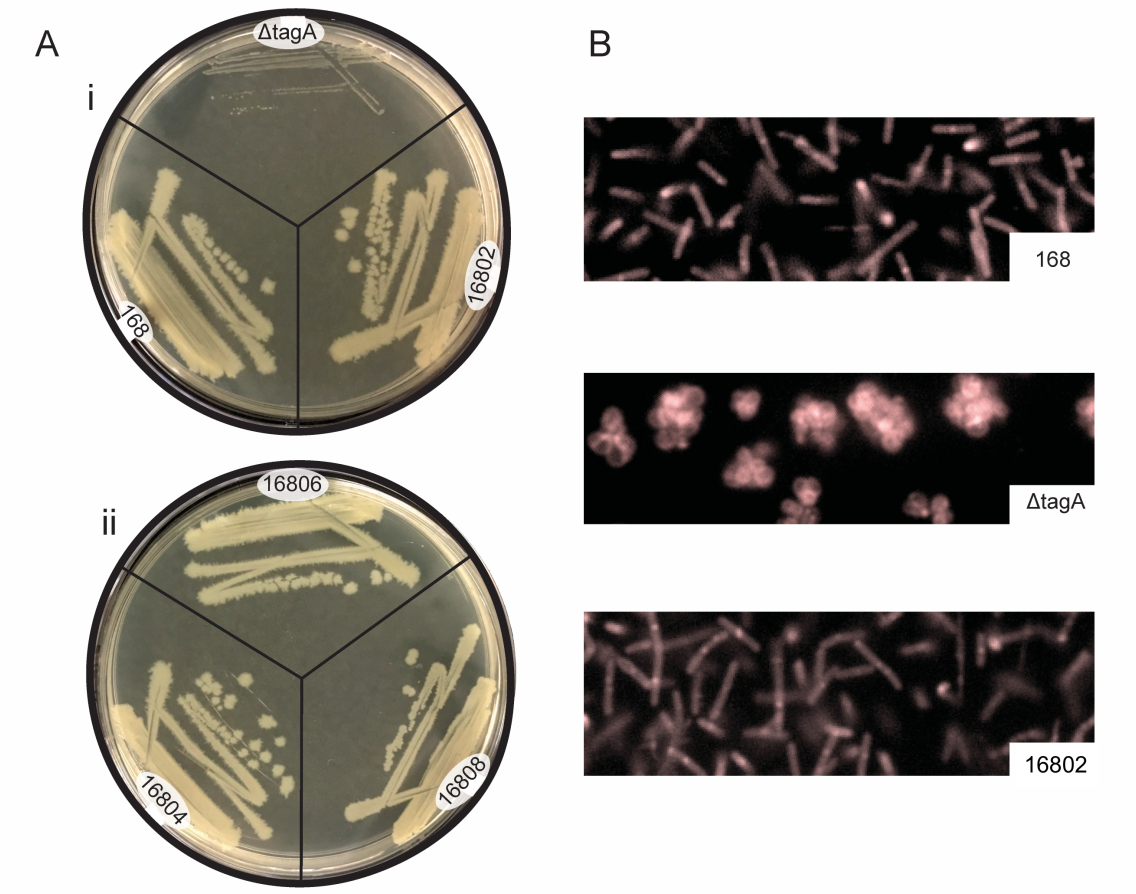

Figure 8: Growth and morphology of *B. subtilis* strains in this study. (A) Images of LB agar plates lacking antibiotic or IPTG of the indicated strains. Cells were streaked out from glycerol stocks onto LB agar plates containing the necessary antibiotics and grown overnight at 37°C . Cells from antibiotic plates were streaked onto LB agar without antibiotic and allowed to grow overnight at 37°C. Strains represented include (*i)* 168, *tagA::*erm (ΔtagA), *thrC::tarA tagA*::spec (16802) *(ii) amyE::tarA tagA*::neo (16804), *thrC::tagA tagA::*spec (16806), and *thrC::tarA tagA*::spec pMAP65 (16808). See Table I for strain details. All strains appear to have normal colony morphology in the absence of IPTG except strain ΔtagA, which is expected. (B) Fluorescent confocal microscopy using Nile Red to visualize the membrane. *B. subtilis* 168 (top panel) appears as rod-shaped cells while ΔtagA (middle panel) appears as clumps of multiple spherical cells. Strain 16802 lacking *tagA* with *tarA* under control of the IPTG promoter appears identical to strain 168 in size and morphology.

Acetylmannosamine transferase that produces the "linkage unit" of WTA and is an attractive drug target (Lee 2010, Farha 2013, Brown 2013).

Results

Strain 16802 construction. In strain 16802, WTA production is dependent on the activity of the *S. aureus* TarA (^{Sa}TarA) as the functionally homologous *B. subtilis* TagA enzyme has been genetically deleted (Table I). ^{Sa}*tarA* was cloned into the *thrC* locus and the endogenous *tagA* was subsequently knocked out using a spectinomycin resistance cassette (see *Materials and Methods*). The strain was characterized using RT-qPCR and WTA purification and visualization.

We were able to produce and maintain *B. subtilis* strain 16802 lacking its endogenous *tagA* gene with *tarA* under control of the P_{spac} promoter at the *thrC* locus. Despite colony PCR experiments indicating that we had produced a strain lacking endogenous *tagA, B. subtilis* strain 16802 appeared to grow with no hindrance to growth rate or colony morphology in the absence of IPTG (Figure 8A*i)*. Strain 16806, identical to 16802 but with ^{Bs}*tagA* under control of the P_{spac} promoter, also appeared to grow normally in the absence of IPTG (Figure 8A*ii)*. This prompted us to attempt more stringently-regulated expression systems.

Attempts to better control tarA *expression.* Characterization of 16802 revealed that *tarA* was being expressed without induction by IPTG (*vide infra*). To address the issue of high basal expression, we created two more strains. We first attempted to increase repression by increasing the repressor-to-operator ratio. We transformed strain 16802 with plasmid pMAP65, an autonomous multi-copy plasmid that constitutively expresses LacR (Table I). After performing colony PCR to verify plasmid transformation, we observed no change in colony growth rate or morphology on LB agar plates and did not pursue the strain further (Figure 8A*ii)*. Most IPTG-inducible promoters contain only one *lac* operator site that physically blocks the polymerase and

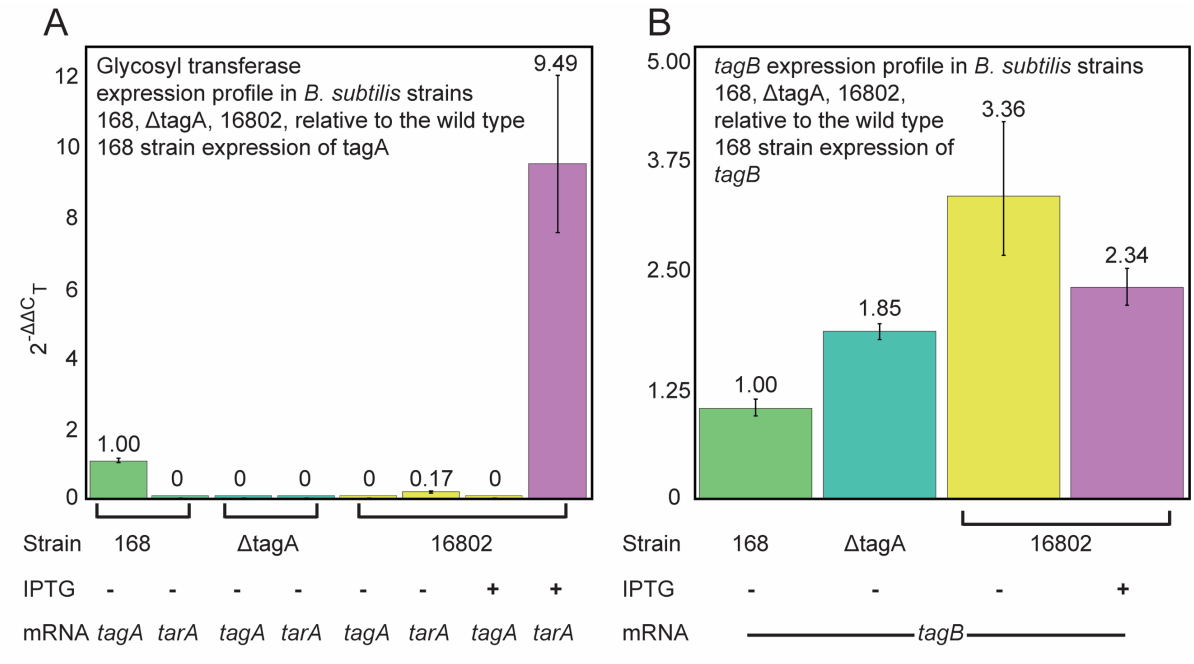

Figure 9: RT-qPCR data for *B. subtilis* strains. Data was analyzed using a relative quantification method with *gyrB* serving as an internal control. (A) Glycosyl transferase expression profile in *B. subtilis* strains. qPCR results indicate that *tarA* is measurably expressed without the presence of IPTG. Data was processed using the $2^{-\Delta\Delta CT}$ method using 168 *tagA* as the calibrator gene. *tarA* expression levels increase as a result of IPTG induction by 9 fold. (B) *tagB* expression profile in *B. subtilis* strains. qPCR results suggest that *tarB* is being transcribed at or above wild type strain 168 levels, implying that despite genetic manipulation, the WTA biosynthesis pathway is intact. Error bars represent one standard deviation above and below the average of a triplicate data set.

abates fidelity, preventing transcription. However, the *lac* repression system contains two non-contiguous operator sites. The two sites are each bound by their own LacR dimer and the two dimers oligomerize to create a dimer of dimers, thereby looping DNA and physically occluding the operator from polymerase binding. Another strain was therefore constructed that contains two *lacO* sites. ^{Sa}*tarA* was subcloned into plasmid pDR110, which contains two operators, then transformed into *B. subtilis* to make strain 16804 (Table II). Strain 16804 maintained wild type morphology similar to strain 168 and 16802 (Figure 8A*ii*). We concluded that these strains were not able to completely halt *tarA* expression and focused our characterization efforts on strain

16802. However, these strains should be studied and considered for HTS as they may produce fewer TarA molecules.

Genetic characterization of strain 16802. To ensure that no *tagA* was being expressed in strain 16802 (*thrC::tarA tagA::*spec), we performed reverse transcription-quantitative polymerase chain reaction (RT-qPCR). We assessed *tagA, tagB,* and *tarA* transcript levels (Figure 9). RT-qPCR indicated that strain 16802 had no detectable *tagA* transcript. Also in strain 16802, the absence of IPTG allowed basal transcription levels of *tarA* at 17% of wild type *tagA* transcription levels in strain 168 (Figure 9A, bars 1 and 6). RT-qPCR indicated that *tagB* was being transcribed at or above wild type levels in all strains, suggesting that the WTA biosynthetic pathway remains intact other than the absence of endogenous TagA (Figure 9B).

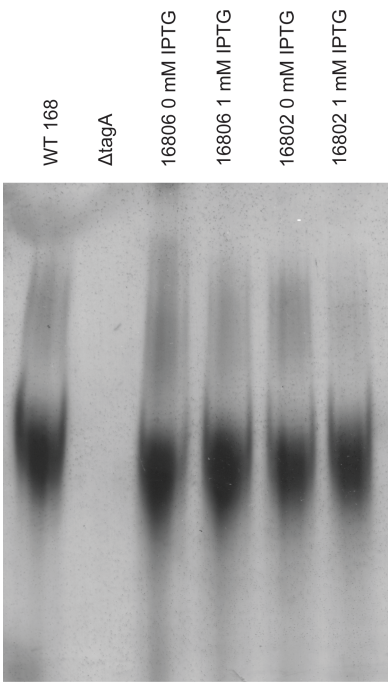

Figure 10: WTA acid purification and visualization using alcian blue-silver staining. Each lane represents a discrete strain with or without IPTG, as indicated. WTA are robustly produced in all strains regardless of IPTG, indicating that ^{Sa}TarA functions in *B. subtilis*. WTA purification was performed in duplicate and this gel is representative of the general results.

Characterization of surface-displayed WTA. We next purified WTA from strains 168, Δ*tagA*, 16802, and 16806 to confirm that the production of WTA was maintained. The Δ*tagA* strain of *B. subtilis* has been previously characterized and lacks the ^{Bs}*tagA* gene and cannot produce WTA. While the 168 positive control strain showed a uniform smear, the negative control strain Δ*tagA* showed a complete absence of smearing or other marks when developed with the alcian blue-silver stain method (Figure 10). Purification of WTA from strains 16802 and 16806

appeared to be robust and WTA polymer length appears unaffected by TarA *trans*-complementation. Though strains 16802 and 16806 utilize IPTG-inducible promoters, the intensity of the bands appears unaffected by IPTG presence.

Strain 16802 is a useful tool for HTS because it relies on ^{Sa}TarA for its rod morphology. To assess whether *B. subtilis* could be visualized using HTS, we plated strains 168, Δ*tagA,* and 16802 in 384-well plates and imaged cells in the presence of the lipophilic stain Nile Red on a confocal microscope capable of HTS. The marked difference in cell morphology is easily visible between strain Δ*tagA* and 168 or 16802. However, there is no visible difference between the morphologies of strain 168 and 16802 when visualized using methods appropriate for HTS (Figure 8B, top and bottom panels). These results indicate that WTA are produced to adequately satisfy the needs of the bacterium to properly perform cell wall biogenesis and complete replication.

Discussion

^{Sa}TarA replaces the glycosyltransferase activity of ^{Bs}TagA and produces a strain displaying WTA on the peptidoglycan. RT-qPCR data indicates that in strain 16802, TarA is expressed in the absence of TagA with or without IPTG, implying that the TarA protein can be present at all times in the cell. High basal expression of TarA in the absence of TagA in strain 16802, which grows with colonies that resemble wild-type strain 168, led us to hypothesize that WTA production should be intact regardless of IPTG.

WTA purification confirmed this hypothesis, showing a robust yield of WTA hydrolyzed from cell wall material under conditions lacking IPTG. Interestingly, the intensity of the bands appears to be similar regardless of IPTG presence. Though impossible to assume any absolute protein concentration, it is interesting to note that very little ^{Sa}*tarA* transcript yields enough

protein to completely satisfy cellular needs for WTA production. This suggests either a high translation rate of the ^{Sa}*tarA* gene or a highly active enzyme, or both. Previous *in vitro* studies of the ^{Bs}TagA enzyme indicate a rapid turnover rate, which is consistent with these results that suggest that a low abundance of ^{Sa}TarA is sufficient for normal bacterial growth (Y. G. Zhang 2006).

Strain 16802 is an exciting new system for studying the activity of ^{Sa}TarA in the cellular environment. Utilizing the morphological dependence of *B. subtilis* on WTA production, we can employ HTS for inhibitors of ^{Sa}TarA by monitoring cell morphology using confocal microscopy. We have shown that *B. subtilis* cells can be rapidly and clearly imaged in a 384-well plate format and that the characteristic rod and spherical morphologies are easily discernable. This HTS can identify inhibitors of the TarA enzyme that will mitigate bacterial virulence and have a significant impact on bacterial infection treatments.

Materials and Methods

B. subtilis strains and media. B. subtilis 168 was grown in LB Broth (Fisher BP9723-500). Minimal media and the protocol used to make competent *B. subtilis* cells is as previously described by Anagnostopoulos and Spizizen (Anagnostopoulos C. 1961) with some modifications (Molecular Biological Methods for Bacillus 1990). When necessary, supplements were included at the following concentrations: erythromycin (1 μg mL^{-1}), spectinomycin (100 μg mL^{-1}), chloramphenicol (7.5 μg mL^{-1}), Isopropyl β-D-1-thiogalactopyranoside (IPTG) (1mM). E. coli XL10 Gold strain (Agilent #200314) used for sub-cloning was maintained on LB agar plates with ampicillin (100 μg mL^{-1}) as required.

Cloning. All bacterial strains are listed in Table 1 and plasmids used are listed in Table 2. Briefly, *B. subtilis* 168 was transformed with the integrative plasmid pBL113::*tarA* containing *S.*

aureus tarA under control of the IPTG inducible P_{spac} promoter using erythromycin on LB Agar plates as a selection marker. Individual colonies were streak purified twice and patched onto minimal media plates lacking threonine to verify double crossover and threonine auxotrophy. Double-crossover events were also verified using colony PCR and primers 49431280 and 49431281 (data not shown). Colony PCR was performed using Apex Red mastermix (Ampliqon 180301). Endogenous tagA was knocked out via transformation with a linear PCR product of the spectinomycin cassette amplified from p*tagA::spec* using primers 49617486 and 49617611, including approximately 1 kb of genomic DNA flanking the *tagA* gene on either side. Cells were plated on LB agar containing spectinomycin and IPTG. As *tagA* and *tagB* are transcribed on the same operon, a stem-loop structure engineered into the pIC56 plasmid was removed to ensure transcription through the *tagB* gene. The stem loop was removed using the Gibson assembly protocol (NEB #E2611S) and primers 49617611, 49617486, 49671911, and 49671910. Deletion of *tagA* was verified using colony PCR and primers 49671530 and 49540570, followed by sequencing of the PCR product (Laragen Inc., Los Angeles, CA). pIC56 resistance was switched from spectinomycin to neomycin using primers 50390903, 50390904, 50390809, and 50391592.

Reverse transcription-quantitative polymerase chain reaction. Cultures were grown to approximately $OD_{600} = 0.5$ and centrifuged at 4000 rcf for ten minutes to collect cells. Media was aspirated and RNA was isolated using Ribopure™ RNA purification kit for bacteria (Thermofisher #AM1925) according to manufacturer's recommendations. Purified RNA was stored at -80°C. RNA concentration was measured using a Thermofisher NanoDrop™ 2000 at 260 nm. cDNA was synthesized using 500-1000 µg of RNA and the Superscript III First-Strand Synthesis System (Thermofisher #18080051) as recommended by the manufacturer using the primers listed in Table II. 1 µL of cDNA produced from reverse transcription was added to 19

µL of iTaq Universal SYBR® Green Supermix with appropriate primers listed in Table II at 300 nM (BioRad #172-5120). Purified RNA diluted identically to RNA used for cDNA synthesis was used as a negative control template to verify the absence of contaminating gDNA. qPCR experiments were conducted using a CFX Connect Real-time PCR Detection System (BioRad #1855201). Data was analyzed using the $2^{-\Delta\Delta CT}$ method as previously described, using *gyrB* as an internal control (Livak 2001).

Fluorescence Microscopy. Overnight cultures were grown in LB Broth with appropriate antibiotics. Cultures were inoculated at OD_{600} = 0.05 and grown to mid-log phase. Cells were spun at 3000g for ten minutes, washed once with sterile PBS, and re-suspended in fresh, sterile PBS. Each suspension of cells was then run through a sterile 5 µm strainer (PluriSelect #43-50005-03) to break apart cellular rafts. Cell density was measured and diluted to OD = 0.01 using sterile PBS. To image the cell membrane, Nile Red (ThermoFisher N1142) was added to a final concentration of 1 µg mL^{-1}. 50 µL aliquots of cell suspensions were immediately distributed into 384-well plates (E&K Scientific EK-30091) and spun at 1000g for ten minutes. Images were captured with the Molecular Sciences ImageXpress Micro Confocal High-content Imaging System using 552/636 nm excitation/detection wavelengths.

WTA polyacrylamide gel electrophoresis. Wall teichoic acid isolation and alcian blue-silver stained gel development were as previously described with some exceptions (Wolters 1990, Meredith 2008, Mann 2016). Cells grown overnight were spun at 3000 g for 15 minutes and washed once with fresh LB Broth. Cultures were harvested and normalized by OD_{600}. 25 µL purified WTA samples were prepared by diluting pure WTA Extract 1:4 in loading buffer (50% glycerol in running buffer, trace bromophenol blue) and loaded on 20% polyacrylamide TBE gels (Life Technologies EC6315BOX) and run until the tracking dye reached the bottom of the

gel (approximately 160 minutes) at 180V and 4°C in running buffer (0.1M Tris-base, 0.1M tricine, pH 8.2 with acetic acid). To prevent alcian blue precipitation, the gel was removed from its cassette and washed twice in wash buffer (10% acetic acid, 25% ethanol, 65% nano-pure water) for 5 and 10 minutes, followed by a 5 minute wash in water. The gel was soaked in 1 mg mL^{-1} alcian blue in water for 40 minutes and washed briefly with nanopure water before a 2 hour de-stain in nanopure water. The gel was soaked in an oxidizing buffer (3.4 mM potassium dichromate, 3.2 mM nitric acid) for seven minutes and quickly washed with water several times. The gel was placed in 12mM silver nitrate for 25 minutes approximately 20 cm below a 100W incandescent light bulb. The silver nitrate was aspirated and the gel washed quickly several times with water. Developing buffer (280mM sodium carbonate, 6mM formaldehyde) was washed over the gel, almost immediately turned brown and was aspirated. More developing buffer was added and aspirated when the solution turned brown. The gel was allowed to incubate in fresh developing buffer until the bands were adequately dark with minimal background staining (less than one minute). The gel was immediately washed with 100mM acetic acid to stop development and then stored in nanopure water.

Table I: Bacterial strains and plasmids used in chapter II		
***B. subtilis* strains**		
168	*trpC2*	1-7
16801	*thrC::tarA* 168 transformed with pBL113::*tarA*	This work
16802	*thrC::tarA tagA*::spec 16801 transformed with ptagA::spec	This work
16803	*amyE::tarA* 168 transformed with p*DR110*::*tarA*	This work
16804	*amyE::tarA tagA*::neo 16803 transformed with p*tagA::neo*	This work
16805	*thrC::tagA* 168 transformed with pBL113::*tagA*	This work
16806	*thrC::tagA tagA::*spec 16805 transformed with ptagA::spec	This work
16808	*thrC::tarA tagA*::spec pMAP65 16802 transformed with pMAP65	This work
ΔtagA	*168* transformed with an Erm cassette to remove *tagA*	(M. A. D'Elia 2009)
Plasmids		
pBL113	Erm^R expression plasmid with P_{spac} promoter, integrates at *thrC* locus	B. Lazzazera, UCLA (unpublished)
pIC56	Integrative cloning plasmid	(Steinmetz 1994)
pMAP65	Autonomous plasmid constitutively expresses LacR protein	(Dervyn 1998)
pDR110	Plasmid containing P_{spac} promoter with to *lac* operators	D. Rudner, Harvard Medical School (unpublished)
pDR110::*tarA*	Plasmid pDR110 that expresses *tarA in B. subtilis*	This work
pBL113::*tarA*	pBL113 plasmid containing *tarA*	This work
p*tagA*::*spec*	pIC56 derived $spec^R$ cassette flanked by tagA-flanking genomic *B. subtilis* DNA	This work
ptagA::neo	pIC56 derived neo^R cassette flanked by tagA-flanking genomic B. subtilis DNA	This work

Table II: Primers used chapter II		
Primer ID	Description	Nucleotide sequence
49431281	Colony PCR at *thrC* locus Fwd	ggcctgctccgctgagag
49431280	Colony PCR at *thrC* locus Rev	gaaaattgctcatgtaaatcatcaaaaag
49617611	Spectinomycin resistance cassette amplification for stem loop removal and Gibson Assembly Fwd	cactgtcatagcaggctcttc
49617486	Spectinomycin resistance cassette amplification for stem loop removal and Gibson Assembly Rev	actcaccgcatgtaaaga
49671911	pIC56 linearization for stem loop removal and Gibson Assembly Fwd	ccatttatttgaaagttttgtttctaattgagagaagtttctatag
49671910	pIC56 linearization for stem loop removal and Gibson Assembly Rev	ctatagaaacttctctcaattagaaacaaaactttcaaataaatgg
50390903	pIC56 linearization to switch spec to neomycin resistance and Gibson Assembly Fwd	catccatttatttgaaagttttgtttcaaaatggtatgcgttttgacac
50390904	pIC56 linearization to switch spec to neomycin resistance and Gibson Assembly Rev	atatgaacataatcaacgaggtgaaatcatgaatggaccaataataatgactagagaag
50390809	Neomycin amplification for Gibson Assembly Fwd	aaacaaaactttcaaataaatggatg
50391592	Neomycin amplification for Gibson Assembly Rev	gatttcacctcgttgattatgttcatataaag
49617486	p*tagA::spec* PCR linearization for transformation Fwd	Actcaccgcatgtaaaga
49617611	p*tagA::spec* PCR linearization for transformation Rev	cactgtcatagcaggctcttc
49671530	*tagA* knockout colony PCR Fwd	cgtaccggatagtttctccatct
49540570	*tagA* knockout colony PCR Rev	gtaccatgacctccatgtttc
49866832	*tarA* RT-qPCR Fwd	cgtttgcacatcatcacg
49866833	*tarA* RT-qPCR Rev	agggaatcccatacctac
49866829	*tagA* RT-qPCR Fwd	cgcaggttattcagacg
49866856	*tagA* RT-qPCR Rev	gaggataccctaaagctacg
49924897	*tagB* RT-qPCR Fwd	ctgttggctcagaagagatgg
49924912	*tagB* RT-qPCR Rev	tcggtaataagggtctgttaaagg
49983279	*gyrB* RT-qPCR Fwd	ctaagcggagatgacgtaagg
49983280	*gyrB* RT-qPCR Rev	tccgtgcttctgagttgc

References

Anagnostopoulos C., Spizizen J. 1961. "Requirements for transformation in Bacillus subtilis." *Journal of Bacteriology* 741-746.

Baddiley, J. 1969. "Structure , Biosynthesis , and Function of Teichoic Acids." *Journal of the American Chemical Society* 98–105.

Bhavsar, A. P., Truant, R., & Brown, E. D. 2005. "The TagB protein in Bacillus subtilis 168 is an intracellular peripheral membrane protein that can incorporate glycerol phosphate onto a membrane-bound acceptor in vitro." *Journal of Biological Chemistry* 36691–36700.

Brown S, Santa Maria JP, Walker S. 2013. "Wall Teichoic Acids of Gram-Positive Bacteria." *Annual review of microbiology* 092412-155620. .

Brown, S., Santa Maria JP., Walker S. 2013. "Wall Teichoic Acids of Gram-Positive Bacteria." *Annual review of microbiology* 092412-155620.

Campbell, J. 2012. "High-throughput assessmet of bacterial growth inhibition by optical density measurements." *Current Protocols in Chemical Biology* 1-20.

Campbell, J., Singh, AK., Santa Maria, JP., Kim, Y., Brown, S., Swoboda, JG., Walker, S. 2011. "Synthetic Lethal Compound Combinations Reveal a Fundamental Connection between Wall Teichoic Acid and Peptidoglycan Biosyntheses in Staphylococcus aureus." *ACS Chemical Biology* 106–116.

Cascioferro, S., Totsika, M., & Schillaci, D. 2014. "Sortase A: An ideal target for anti-virulence drug development. Microbial Pathogenesis." *Microbial Pathogenesis* 105–112.

Center for Disease Control. 2014. "CDC.org." July 14. Accessed May 2, 2017. http://cdc.gov/drugresistance/threat-report-2013/.

Chan, A. H., Wook, S., Ethan, Y., Amer, B. R., Sue, C. K., Wereszczynski, J., Clubb, R. T. 2017. "NMR structure-based optimization of Staphylococcus aureus sortase A pyridazinone inhibitors." *Wiley Drug & Design* 1–18.

Chan, Y. G. Y., Frankel, M. B., Dengler, V., Schneewind, O., Missiakas, D. 2013. "Staphylococcus aureus Mutants Lacking the LytR-CpsA-Psr Family of Enzymes Release Cell Wall Teichoic Acids into the Extracellular Medium." *Journal of Bacteriology* 4650–4659.

Comolli, J. C., Hauser, A. R., Waite, L., Whitchurch, C. B., Mattick, J. S., & Engel, J. N. 1999. "Pseudomonas aeruginosa Gene Products PilT and PilU Are Required for Cytotoxicity In Vitro and Virulence in a Mouse Model of Acute Pneumonia." *Infection and Immunity* 3625–3630.

Dervyn, E., Entian, K., Mcgovern, S., Ehrlich, S. D., Bruand, C., Goethe, J. W. 1998. "PcrA is an essential DNA helicase of Bacillus subtilis fulfilling functions both in repair and rolling-circle replication." 61–273. .

D'Elia, M. A., Henderson, J. A., Beveridge, T. J., Heinrichs, D. E., Brown, E. D. 2009. "The N-acetylmannosamine transferase catalyzes the first committed step of teichoic acid assembly in Bacillus subtilis and Staphylococcus aureus." *Journal of Bacteriology* 4030–4034.

D'Elia, M. A., Millar, K. E., Beveridge, T. J., Brown, E. D. 2006. "Wall teichoic acid polymers are dispensable for cell viability in Bacillus subtilis." *Journal of Bacteriology* 8313–8316.

D'Elia, M. A., Pereira, M. P., Chung, Y. S., Zhao, W., Chau, A., Kenney, T. J., Brown, E. D. 2006. "Lesions in teichoic acid biosynthesis in Staphylococcus aureus lead to a lethal

gain of function in the otherwise dispensable pathway." *Journal of Bacteriology* 4183–4189.

Farha, M. A., Leung, A., Sewell, E. W., D'Elia, M. A., Allison, S. E., Ejim, L., Brown, E. D. 2013. "Inhibition of WTA synthesis blocks the cooperative action of pbps and sensitizes MRSA to B-lactams. ." *ACS Chemical Biology* 226-233.

Fittipaldi, N., Sekizaki, T., Takamatsu, D., Aulock, S. Von, Draing, C., Marois, C., Avicoles, R. 2008. "D -Alanylation of Lipoteichoic Acid Contributes to the Virulence of Streptococcus suis ." *Infection and Immunity* 3587–3594.

Formstone, A., Carballido-López, R., Noirot, P., Errington, J., Scheffers, D. J. 2008. "Localization and interactions of teichoic acid synthetic enzymes in Bacillus subtilis." *Journal of Bacteriology* 1812–1821.

Heckels, B. J. E., Lambert, P. A., Baddiley, J. 1977. "Binding ofMagnesium Ions to Cell Walls of Bacillus subtilisW23 containing Teichoic Acid or Teichuronic Acid." *Biochemistry Journal* 359-365.

Holland, L. M., Conlon, B., Gara, J. P. O. 2011. "Mutation of tagO reveals an essential role for wall teichoic acids in Staphylococcus epidermidis biofilm development." *Microbiology* 408–418.

Labroli, M. A., Caldwell, J. P., Yang, C., Lee, S. H., Wang, H., Koseoglu, S., Su, J. 2016. "Discovery of potent wall teichoic acid early stage inhibitors." *Bioorganic and Medicinal Chemistry Letters* 3999–4002.

Lambert, B. P. A., Hancock, I. A. N. C., Baddiley, J. 1975. "The Interaction of Magnesium Ions with Teichoic Acid." 519–524.

Lee, K., Campbell, J., Swoboda, J. G., Cuny, G. D., Walker, S. 2010. "Development of improved inhibitors of wall teichoic acid biosynthesis with potent activity against Staphylococcus aureus. ." *Bioorganic and Medicinal Chemistry Letters* 1767–1770.

Livak, K. J., & Schmittgen, T. D. 2001. "Analysis of relative gene expression data using real-time quantitative PCR and the 2-ddCt Method." *Methods* 402–408.

Maki, H., Yamaguchi, T., Murakami, K. 1994. "Cloning and Characterization of a Gene Affecting the Methicillin Resistance Level and the Autolysis Rate in Staphylococcus-Aureus." *Journal of Bacteriology* 4993–5000.

Mann, P. A., Müller, A., Wolff, K. A., Fischmann, T., Wang, H., Reed, P., Roemer, T. 2016. "Chemical Genetic Analysis and Functional Characterization of Staphylococcal Wall Teichoic Acid 2-Epimerases Reveals Unconventional Antibiotic Drug Targets." *PLoS Pathogens* 1-26.

Marquis, E., Carstensen, L. 1976. "Cation exchange in cell walls of gram-positive bacteria. ." *Canadian Journal of Microbiology* 975-982.

Mazmanian, S. K., Liu, G., Jensen, E. R., Lenoy, E., Schneewind, O. (. 2000. "Staphylococcus aureus sortase mutants defective in the display of surface proteins and in the pathogenesis of animal infections." *Staphylococcus aureus sortase mutants defective in the display of surface proteins and in the pathogenesis of animal infections. Proceedings of the National Academy of Sciences of the United States of America* 5510–5515 .

Mazmanian, S.K., Tonthat, H. 2001. "Sortase-catalysed anchoring of surface proteins to the cell wall of Staphylococcus aureus." *Molecular Microbiology* 1049–1057.

Mazmanian, SK., Liu, G., Jensen, E. R., Lenoy, E., Schneewind, O. (. 2000. "Staphylococcus aureus sortase mutants defective in the display of surface proteins and in the pathogenesis

of animal infections." *Staphylococcus aureus sortase mutants defective in the display of surface proteins and in the pathogenesis of animal infections. Proceedings of the National Academy of Sciences of the United States of America* 5510–5515.

Mazmanian, SK., Tonthat, H. 2001. "Sortase-catalysed anchoring of surface proteins to the cell wall of Staphylococcus aureus." *Molecular Microbiology* 1049–1057.

Meredith, T. C., Swoboda, J. G., Walker, S. Journal of Bacteriology, 190(8),. 2008. "Late-stage polyribitol phosphate wall teichoic acid biosynthesis in Staphylococcus aureus." *Journal of Bacteriology* 3046–3056.

Misawa, Y., Kelley, K. A., Wang, X., Wang, L., Park, W. B. 2015. "Staphylococcus aureus Colonization of the Mouse Gastrointestinal Tract Is Modulated by Wall Teichoic Acid , Capsule , and Surface Proteins." *PLOS Pathogens* 1-21.

Schirner, K., Stone, L. K., & Walker, S. 2011. "ABC Transporters Required for Export of Wall Teichoic Acids Do Not Discriminate between Different Main Chain Polymers." *ACS Chemical Biology.*

Steinmetz, M., Richter, R. 1994. "Plasmids designed to alter the antibiotic resistance expressed by insertion mutations in Bacillus subtilis, through in vivo recombination. ." *Gene* 79–83.

Suzuki, T., Campbell, J., Swoboda, J. G., Walker, S., Gilmore, M. S., Wall, P. U. 2017. "Immunology and Microbiology Role of Wall Teichoic Acids in Staphylococcus aureus Endophthalmitis ." *Immunology and Microbiology* 3187-3192.

Swoboda, J. G., Meredith, T. C., Campbell, J., Brown, S., Suzuki, T., Bollenbach, T., Walker, S. 2009. "Discovery of a Small Molecule that Blocks Wall Teichoic Acid Biosynthesis in Staphylococcus aureus." *ACS Chemical Biology* 875–883.

Weidenmaier, C., Kokai-Kun, J. F., Kristian, S. a, Chanturiya, T., Kalbacher, H., Gross, M., Peschel, A. 2004. "Role of teichoic acids in Staphylococcus aureus nasal colonization, a major risk factor in nosocomial infections." *Nature Medicine* 243–245.

Wolters, P. J., Hildebrandt, K. M., Dickie, J. P., Anderson, J. S. 1990. "Polymer length of teichuronic acid released from cell walls of Micrococcus luteus. Journal of Bacteriology." *Journal of Bacteriology* 5154–5159.

Wu, C., Huang, IH., Chang, C., Reardon-Robinson, ME., Das, A., Ton-That, H. 2014. "Lethality of Sortase Depletion in Actinomyces oris Caused by Excessive Membrane Accumulation of a Surface Glycoprotein." *Molecular Microbiology* 1227–1241.

Wu, X., Paskaleva, E. E., Mehta, K. K., Dordick, J. S., Kane, R. S. 2016. "Wall Teichoic Acids Are Involved in the Medium-Induced Loss of Function of the Autolysin CD11 against Clostridium difficile." *Scientific Reports* 1-11.

Zhang, JH., Chung, T., Oldenburg, K. 1999. "A Simple Statistical Parameter for Use in Evaluation and Validation of High Throughput Screening Assays." *Journal of Biomolecular Screening* 67-73.

Zhang, Y.H., Ginsberg C, Yuan Y, Walker S. 2006. "Acceptor Substrate Selectivity and Kinetic Mechanism of Bacillus subtilis TagA." *Biochemistry* 10895-10904.